

Self Similarity Image Registration Based on Reorientation of the Hessian

Zhang Li¹, Lucas J. van Vliet¹, and Frans M. Vos^{1,2}

¹ Quantitative Imaging Group, Department of Imaging Science and Technology,
Delft University of Technology, 2628CJ Delft, The Netherlands

`z.li-1@tudelft.nl`

² Department of Radiology, Academic Medical Center,
1105AZ Amsterdam, The Netherlands

Abstract. The modality independent neighbourhood descriptor (MIND) is a local registration metric that is based on the principle of self-similarity. However, the metric requires recalculation of the self similarity during registration as this inherently changes during image deformation. We propose a self similarity registration method based on the Hessian (HE) that efficiently deals with the recalculation issue. The representation of the local self-similarity via the Hessian enables keeping it up to date during deformation. As such, the registration procedure is efficient and not prone to fall in local minima. We have shown that reorienting the hessian gives a significant improvement ($p < 0.05$) over leaving the reorientation out. Our technique also has a better performance over the existing MIND method on the DIR-Lab dataset as well as on abdominal MRI datasets albeit not significant. Ultimately, we will use the technique to quantify Crohn's disease severity based on the relative contrast enhancement in registered images.

Keywords: Image registration, hessian reorientation, Crohn's disease.

1 Introduction

Medical image registration is widely used for finding correspondence between images. Sum of square differences (SSD) and normalized cross covariance (NCC) are often applied for registering images from the same modality. Alternatively, mutual information (MI) is frequently used to deal with multi-modal image registration problems [1–3].

The above, basic similarity metrics are based on global measurements and in principle do not model spatial variance. However, such variance is known influence the robustness of non-rigid registration tasks [4]. Accordingly, Gorbunova et al. [5] proposed a local mass preserving SSD technique for lung CT registration. Likewise, Song et al. [6] used local cross correlation to accommodate inhomogeneities of CT scans. Furthermore, Loeckx et al. [4] proposed a conditional implementation of MI, introducing a spatial dimension into the 3D joint histogram. More approaches combining spatial information into MI can be found in [7–9].

It has been noticed [10] that such local estimation can be difficult, though, due to many false local optima in non-rigid registration. An alternative way of incorporating spatial variance was based on structural representations of images. For instance, gradient can be used to find correspondence of images [11, 12]. Moreover, Heinrich et al. [13] proposed a method that relied on orientation information derived from the structure tensor. More recently, the same group [10] introduced the modality independent neighbourhood descriptor (MIND) that is based on the principle of self-similarity. Essentially, this technique assumes that the local image structure is shared by the images to be registered. The method yielded reliable registration results accross different image modalities and better performance than other state-of-the-art approaches. However, the metric requires recalculation of the self similarity during registration as this inherently changes during image deformation.

We propose a self similarity registration method based on the Hessian (HE) that efficiently deals with the recalculation issue. Our method relies on a reorientation strategy adapted from diffusion tensor image registration [14]. A key novelty is that the reorientation of Hessian (ROHE) is integrated in the registration optimization. We compare our procedure with the MIND method on the same dataset from DIR-Lab [15] since MIND is also a self-similarity based method and its performance was previously tested on that dataset. Additionally, we evaluate the technique on abdominal pre- and postcontrast MRI datasets. Ultimately, it is our objective to employ the method to quantify the amount of contrast enhancement in those images, which is known to reflect Crohn’s disease severity.

2 Methods

2.1 Modality Independent Neighbourhood Descriptor (MIND)

The MIND descriptor is formally defined as :

$$\text{MIND}(I, \mathbf{x}_c, \mathbf{r}) = \frac{1}{n} \exp\left(-\frac{D_p(I, \mathbf{x}_c, \mathbf{x}_{c+r})}{V(I, \mathbf{x}_c)}\right) \quad \mathbf{r} \in R \quad (1)$$

in which D_p in (3) is a similarity measure between small patches around a center voxel \mathbf{x}_c respectively a neighbouring voxel \mathbf{x}_{c+r} , both of which are taken from a neighbourhood R . Effectively, MIND yields a vector of size R which represents the local structure information around each center voxel. In (1) n and $V(I, \mathbf{x}_c)$ are normalization terms with n the neighbourhood size and:

$$V(I, \mathbf{x}_c) = \frac{1}{6} \sum_{r \in N} D_p(I, \mathbf{x}_c, \mathbf{x}_{c+r}) \quad (2)$$

Furthermore, the similarity measure D_p is given by:

$$D_p(I, \mathbf{x}_c, \mathbf{x}_{c+r}) = \sum_{p \in P} (I(\mathbf{x}_c + p) - I(\mathbf{x}_{c+r} + p))^2 \quad (3)$$

representing the sum of squared difference (SSD) between two identically shaped patches P .

In essence, MIND maps each voxel onto a self-similarity vector that embeds the local structure. Subsequently, the registration problem is solved by minimizing the sum of absolute differences of MIND measures over two images I and J under a certain deformation function.

2.2 Definition of the Hessian and Reorientation Strategy

An alternative method to measure local structure is based on the Hessian (HE):

$$HE = \begin{bmatrix} I_{xx} & I_{xy} & I_{xz} \\ I_{yx} & I_{yy} & I_{yz} \\ I_{zx} & I_{zy} & I_{zz} \end{bmatrix} \quad (4)$$

The calculation of image derivatives is based Gaussian kernels (width: σ_g). Typically, the HE is sensitive to the linelike structures (even structures). It captures local orientation which is also covered by MIND.

In Diffusion Tensor Image (DTI) registration, tensor reorientation has been incorporated in the registration optimization [14]. Thereby the local orientation can be preserved during the registration and registration efficiency also might be improved. A standard way to do so is the Finite strain (FS) strategy in which a rigid rotation component is calculated by decomposing the deformation gradient:

$$R(\mathbf{x}) = (J(\mathbf{x})J(\mathbf{x})^T)^{-\frac{1}{2}}J(\mathbf{x}) \quad (5)$$

where $R(x)$ in (5) is the rotation matrix in a voxel and $J(x)$ is deformation gradient (i.e. Jacobian) at that voxel. Subsequently, the diffusion tensor $T(x)$ is reoriented by:

$$T'(\mathbf{x}) = R^T(\mathbf{x})T(\mathbf{x})R(\mathbf{x}) \quad (6)$$

Our structural representations make that a reorientation strategy is directly applicable in a new optimization framework. The effect of reorientation on a HE image is illustrated in 2D in Fig.1. It can be seen in the HE image without reorientation (b) that there is a disparity with the 'ground truth' (e), see the white arrows. Instead, the reoriented image (c) from (b) much closer resembles the ground truth (f).

2.3 Registration Framework

Inspired by [10] our similarity metric at each voxel is the mean absolute differences of HE's:

$$S(HE_f(\mathbf{x}), HE_m(\mathbf{x})) = \text{mean}|HE_f(\mathbf{x}) - HE_m(\mathbf{x})|^2 \quad (7)$$

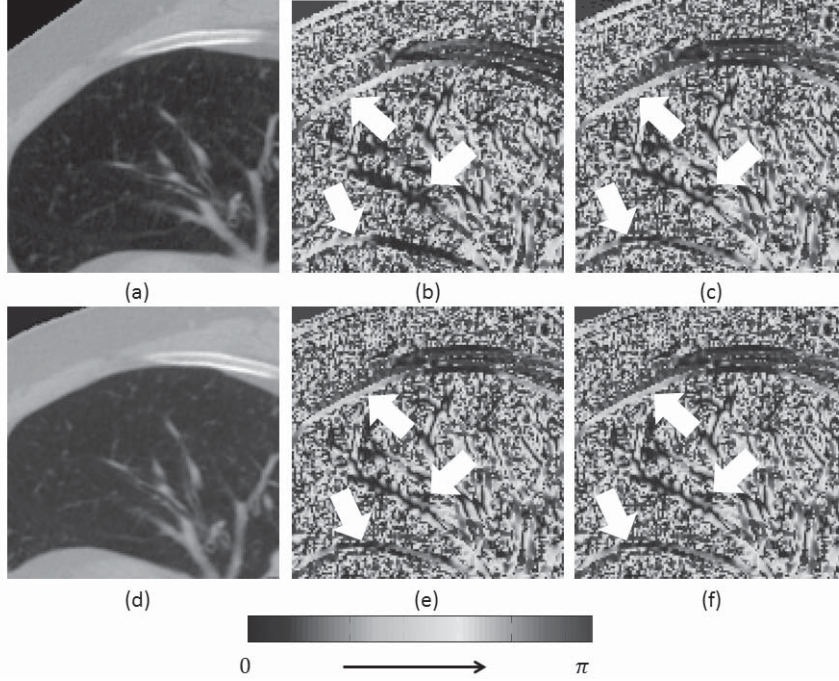


Fig. 1. Illustration of the effect of reorientation on the HE. (a) is an example lung CT image that we rotated by 30 degrees clockwise around the z direction yielding image (d). Images (b)(c)(e)(f) display the orientation of the first eigenvector derived from the Hessian; (b) shows a 30 degrees rotated tensor image derived from image (a) ($\sigma_g = 0.5$ calculated without reorientation) and (e) is the 'ground truth' calculated from (d). (c) is the result after rotation *and* reorientation from (a) and (f) is a duplicate version of (e) just for comparison.

where the $HE_f(\mathbf{x})$ and $HE_m(\mathbf{x})$ are the Hessian in voxel \mathbf{x} from the fixed image and moving image respectively. We map the fixed image and moving image to Hessian space and a Gaussian Newton optimisation scheme was used to minimize following the cost function:

$$\underset{\mathbf{u}}{\operatorname{argmin}} \sum_{\mathbf{x}} \mathcal{S}(HE_f(\mathbf{x}), R(\mathbf{x}+\mathbf{u})^T HE_m(\mathbf{x}+\mathbf{u}) R(\mathbf{x}+\mathbf{u}))^2 + \alpha \operatorname{tr}(\nabla \mathbf{u}(\mathbf{x})^T \nabla \mathbf{u}(\mathbf{x}))^2 \quad (8)$$

where $R(\mathbf{x} + \mathbf{u})$ is the rotation matrix, \mathbf{u} is the deformation field and α is a parameter that weights a regularisation term.

In the optimization step, MIND is recalculated after a certain number of deformation steps (more detail can be found in [10]). In contrast, our approach involving the Hessian enables to incorporate a reorientation term into the cost function and thus cope with the deformation (Equation (8)). The Hessian is only calculated once and the deformation of Hessian is embedded in the optimization.

Table 1. Mean distances(mm) of landmarks in 10 lung CT images: INITIAL is prior to registration; HE give the outcome based on HE registration without reorientation; ROHE are the result if reorientation is included; MIND is the outcome using the MIND framework

Case	1	2	3	4	5	6	7	8	9	10	Mean
INITIAL	4.07	4.40	7.03	9.91	7.51	10.99	11.13	15.06	8.02	7.43	8.56
HE	1.91	1.80	2.30	2.60	3.02	5.13	4.74	9.53	3.14	2.67	3.68
MIND	1.05	1.06	1.23	1.48	1.62	1.61	2.04	3.46	1.37	1.63	1.66
ROHE	1.08	1.06	1.27	1.53	1.56	1.64	1.92	3.26	1.36	1.60	1.62

As such, we can already reckon with an altering self-similarity when determining Gauss-Newton optimization steps (given by the gradient of Equation (8)). By doing so it may be expected that the technique is less prone to convergence in local minima. The interpolation inherent to the registration problem was performed trilinearly in the derivative spaces after which an interpolated Hessian was calculated.

3 Experiments and Results

3.1 DIR-Lab 4D CT

We tested our registration framework based on the HE on the public dataset provided by the DIR-Lab at the University of Texas [15]. This data set consists of thorax CT volumes acquired in inspiration as well as expiration from 10 subjects in which 300 landmarks were annotated by experts. A comparison of our approaches with the MIND approach are collated in Table 1. Thereby, we used $\sigma_g = 0.5$ and $\alpha = 0.1$, all of which were chosen to be comparable to the MIND approach. .

A two sample t-test was used to compare the registration strategies. Particularly, the results of ROHE and MIND are significant improvements over the initial situation as well as registration based on HE without reorientation (all: $p < 0.05$) . ROHE has lower mean distance than MIND, but this difference is not significant. Fig. 2 shows a registration case based on ROHE and MIND. Although the difference in performance is subtle, it can be clearly seen that near the lung boundary ROHE outperforms MIND (see red arrow). Here, MIND appears to converge in a local minimum since increasing the number of steps does not improve the registration outcome. We found similar results on other cases. Additionally, we calculated the sum of absolute intensity differences (SAD) for ROHE and MIND, see Table 2, which shows the same trend.

3.2 Pre-contrast and Post-contrast Abdominal MRI

We applied our algorithms to clinical datasets from [16]. From this dataset we sequentially included the first 5 patients diagnosed with Crohn’s disease . Patients drank 1600ml of a hyperosmolar fluid (Mannitol, 2.5%, Baxter, Utrecht,

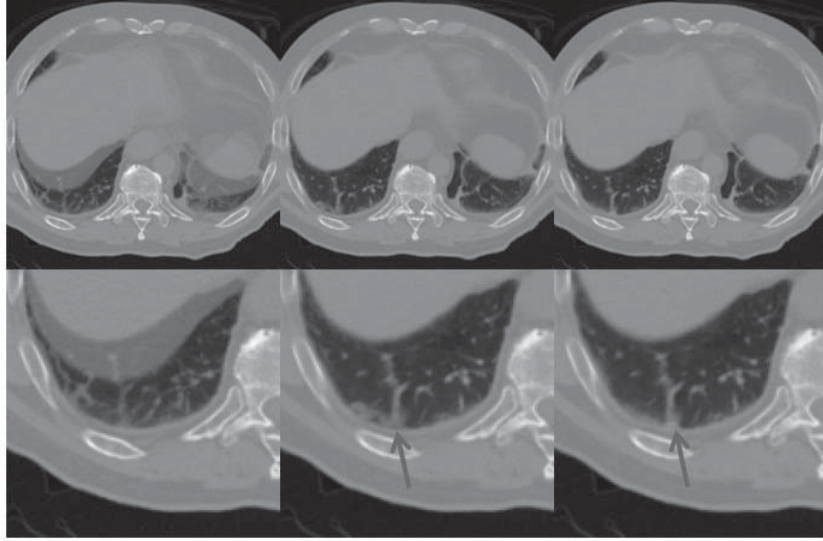


Fig. 2. Registration comparison for case 4. Top is an overview image, bottom shows a detail (as indicated). From left to right are images prior to registration, images registered by MIND and by ROHE, respectively. In all images the inhale phase (fixed image) is displayed in magenta and exhale phase (moving image) is displayed in green.

The Netherlands) 1 hour before acquiring the MRI scans to achieve bowel distention. MR imaging included a high resolution, 3D T1-weighted spoiled gradient echo sequence with fat saturation (pre-contrast MRI), followed by a free-breathing 3D+time Dynamic Contrast Enhanced (DCE)-MRI data acquisition on a 3.0T MRI scanner (Intera, Philips Healthcare, Best, The Netherlands) by a 3D spoiled gradient echo sequence. A contrast agent (Gadovist 1.0 mmol/ml, Bayer Schering Pharma, Berlin, Germany) was injected (0.1 ml/kg bodyweight) during the DCE-MRI acquisition. The DCE sequence was also succeeded by a high resolution, 3D T1-weighted spoiled gradient echo sequence with fat saturation (post-contrast MRI). A bowel relaxant (20 mg, Buscopan, Boehringer, Ingelheim, Germany) was administered to the subjects scans to minimize bowel movement. Registration of the pre and post contrast scans is considered as an important step to quantify disease severity by means of the relative contrast enhancement .

Table 2. Sum of absolute intensity differences ($\times 10^{10}$) prior to registration (INITIAL) and after registration based on MIND and ROHE, respectively

Case	1	2	3	4	5	6	7	8	9	10
INITIAL	6.82	11.03	12.86	10.15	10.75	25.29	29.44	44.46	20.83	23.84
MIND	0.84	1.35	1.15	1.54	1.34	5.92	5.76	5.67	3.08	4.15
ROHE	0.78	1.25	1.07	1.36	1.23	5.47	5.10	5.84	2.76	3.71

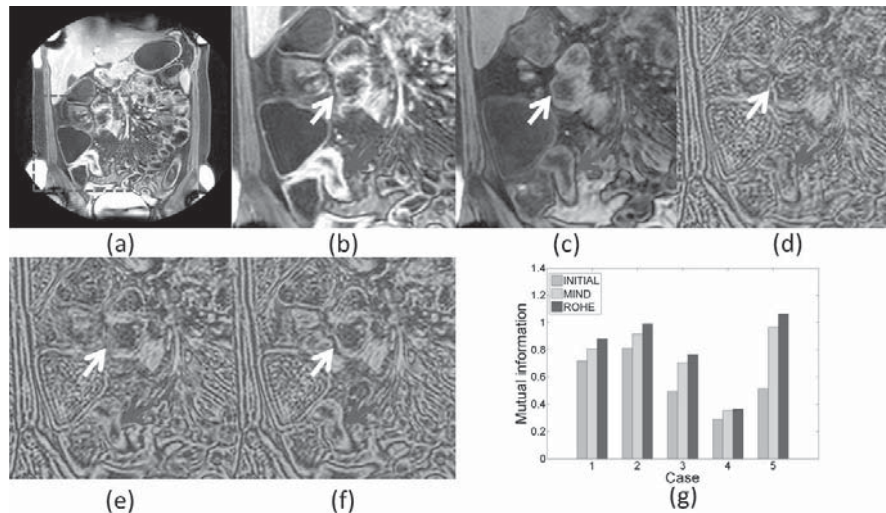


Fig. 3. Registration comparison on abdominal imaging data. (a) is a post-contrast MR image; (b) is sub-regions indicated in (a). (c) is the subregions from pre-contrast MR in same slice position as (b). (d) - (f) are the color mapped versions of the sub-regions prior before registration (d), after registration by MIND (e), ROHE (f), respectively. The locally normalized post-contrast MR sub-region is displayed in magenta and the locally normalized pre-contrast sub-region is displayed in green. (g) quantifies the registration performance via the the mutual information.

The outcome of two registration approaches on a representative example are shown in Fig. 3. The terminal ileum containing Crohn’s disease, is indicated by a red arrow. Fig. 3 (f) results after ROHE based registration yielding best outcome particularly around this region. What is more, Fig. 3 (g) quantifies the registration performance via the the mutual information on all cases (since manually indicated landmarks appeared irreproducible on this data). This figure also reflects that ROHE predominantly gives the best performance .

4 Conclusion

We presented a novel registration procedure based on the Hessian that incorporated a reorientation strategy into the registration optimization. The representation of the local self-similarity as a tensor enabled keeping it up to date during deformation. As such, the registration procedure is efficient and not prone to fall in local minima. We showed that reorienting the hessian gave a significant improvement in registration accuracy ($p < 0.05$) over leaving the reorientation out. Our technique also had a better performance over the existing MIND method on the DIR-Lab dataset as well as on abdominal MRI datasets albeit not significant. In the future we aim to differentiate in the weight given to varying structures (e.g. lines, planes, isotropic structures). Futhermore we will compare our method

with gradient based methods [11, 12]. Ultimately, we will use the technique to quantify Crohn's disease severity based on the relative contrast enhancement in registered images.

References

1. Maes, F., Collignon, A., Vandermeulen, D., Marchal, G., Suetens, P.: Multimodality Image Registration by Maximization of Mutual Information. *IEEE Transactions on Medical Imaging* 16(2), 187–198 (1997)
2. Viola, P., Wells III, W.M.: Alignment by Maximization of Mutual Information. *International Journal of Computer Vision* 24(2), 137–154 (1997)
3. Pluim, J.P.W., Maintz, J.B.A., Viergever, M.A.: Mutual-Information-Based Registration of Medical Images: A Survey. *IEEE Transactions on Medical Imaging* 22(8), 986–1004 (2003)
4. Loeckx, D., Slagmolen, P., Maes, F., Vandermeulen, D., Suetens, P.: Nonrigid Image Registration Using Conditional Mutual Information. *IEEE Transactions on Medical Imaging* 29(1), 19–29 (2010)
5. Gorbunova, V., Lo, P., Ashraf, H., Dirksen, A., Nielsen, M., de Bruijne, M.: Weight Preserving Image Registration for Monitoring Disease Progression in Lung CT. In: Metaxas, D., Axel, L., Fichtinger, G., Székely, G. (eds.) *MICCAI 2008, Part II. LNCS*, vol. 5242, pp. 863–870. Springer, Heidelberg (2008)
6. Song, G., Tustison, N., Avants, B., Gee, J.C.: Lung CT Image Registration Using Diffeomorphic Transformation Models. In: van Ginneken, B., Murphy, K., Heimann, T., Pekar, V., Deng, X. (eds.) *Medical Image Analysis for the Clinic: A Grand Challenge*, pp. 23–32. CreateSpace, Charleston (2010)
7. Yi, Z., Soatto, S.: Multimodal Registration via Spatial-Context Mutual Information. In: Székely, G., Hahn, H.K. (eds.) *IPMI 2011. LNCS*, vol. 6801, pp. 424–435. Springer, Heidelberg (2011)
8. Zhuang, X., Arridge, S., Hawkes, D.J., Ourselin, S.: A Nonrigid Registration Framework Using Spatially Encoded Mutual Information and Free-Form Deformations. *IEEE Transactions on Medical Imaging* 30(10), 1819–1828 (2011)
9. Klein, S., van der Heide, U.A., Lips, I.M., van Vulpen, M., Staring, M., Pluim, J.P.: Automatic Segmentation of the Prostate in 3D MR Images by Atlas Matching Using Localized Mutual Information. *Medical Physics* 35(4), 1407–1417 (2008)
10. Heinrich, M.P., Jenkinson, M., Bhushan, M., Matin, T., Gleeson, F.V., Brady, S.M., Schnabel, J.A.: MIND: Modality Independent Neighbourhood Descriptor for Multi-Modal Deformable Registration. *Medical Image Analysis* 16(7), 1423–1435 (2012)
11. De Nigris, D., Collins, D., Arbel, T.: Multi-Modal Image Registration Based on Gradient Orientations of Minimal Uncertainty. *IEEE Transactions on Medical Imaging* 31(12), 2343–2354 (2012)
12. Li, B., Li, X., Wang, K., Qin, H.: Surface Mesh to Volumetric Spline Conversion with Generalized Polycubes. *IEEE Transactions on Visualization and Computer Graphics* 19(9), 1539–1551 (2013)

13. Heinrich, M.P., Jenkinson, M., Gleeson, F.V., Brady, S.M., Schnabel, J.A.: Deformable Multimodal Registration with Gradient Orientation Based on Structure Tensors. *Annals of the British Machine Vision Association* 5(2), 1–11 (2011)
14. Yeo, B.T., Vercauteren, T., Fillard, P., Peyrat, J.M., Pennec, X., Golland, P., Ayache, N., Clatz, O.: Dt-refind: Diffusion Tensor Registration with Exact Finite-Strain Differential. *IEEE Transactions on Medical Imaging* 28(12), 1914–1928 (2009)
15. Castillo, R., Castillo, E., Guerra, R., Johnson, V.E., McPhail, T., Garg, A.K., Guerrero, T.: A Framework for Evaluation of Deformable Image Registration Spatial Accuracy Using Large Landmark Point Sets. *Physics in Medicine and Biology* 54(7), 1849–1870 (2009)
16. Ziech, M., Lavini, C., Caan, M., Nio, C., Stokkers, P., Bipat, S., Ponsioen, C., Nederveen, A., Stoker, J.: Dynamic Contrast-Enhanced MRI in Patients with Luminal Crohn’s Disease. *European Journal of Radiology* 81(11), 3019–3027 (2012)